Article

Discovery Medicine 2025; 37(202): 2579–2588
https://doi.org/10.24976/Discov.Med.202537202.216

PHLDA2 Drives Malignant Progression in Lung Adenocarcinoma via ELK1-Mediated Transcriptional Activation

Fei Ming[1,*], DaiPing Zhang[2]

[1]Department of Thoracic Surgery, Hubei Cancer Hospital, Tongji Medical College, Huazhong University of Science and Technology, 430070 Wuhan, Hubei, China
[2]Department of Cardiac Function, Hubei Cancer Hospital, Tongji Medical College, Huazhong University of Science and Technology, 430070 Wuhan, Hubei, China
*Correspondence: Mingfei_666@163.com (Fei Ming)
Submitted: 23 June 2025 Revised: 1 September 2025 Accepted: 28 September 2025 Published: 20 November 2025

Background: Lung adenocarcinoma (LUAD) is characterized by a high propensity for metastasis and poor patient outcomes, along with reduced survival rates. This study aims to investigate the role of pleckstrin-homology-like domain family-A member 2 (PHLDA2) in the progression of LUAD and its transcriptional regulation by the ETS-like-1 protein (ELK1).
Methods: PHLDA2 expression was analyzed in The Cancer Genome Atlas-Lung Adenocarcinoma (TCGA-LUAD) (gene expression profiling interactive analysis (GEPIA)) and validated in LUAD cell lines using Western blot (WB) analysis. Functional analyses, including the counting kit-8 (CCK-8) proliferation curves, Transwell migration/invasion, apoptosis, and cisplatin half-maximal inhibitory concentration (IC_{50}) determination, were performed after silencing PHLDA2 (siPHLDA2). Additionally, chromatin immunoprecipitation (ChIP)-quantitative polymerase chain reaction (qPCR) and dual-luciferase reporter assays were used to evaluate ELK1's binding and promoter activation.
Results: PHLDA2 was significantly upregulated in LUAD tumors compared to normal lung tissues ($p < 0.05$), and high PHLDA2 expression was associated with shorter overall survival (Kaplan–Meier, $p = 0.02$). Silencing PHLDA2 reduced proliferation, reversed epithelial-mesenchymal transition (EMT), diminished migration/invasion, and increased cisplatin sensitivity ($IC_{50} \approx$ 16 µM vs. $\approx$ 36 µM in controls). ELK1 bound a –420 bp motif in the PHLDA2 promoter and enhanced its transcription (~3-fold).
Conclusion: These results suggest that the ELK1-PHLDA2 axis promotes LUAD malignancy and chemoresistance and may represent a potential therapeutic target, warranting *in vivo* and clinical validation.

Keywords: PHLDA2; ELK1; lung adenocarcinoma; EMT; cisplatin sensitivity

Introduction

Lung adenocarcinoma (LUAD), the most prevalent subtype of non-small-cell lung cancer (NSCLC), is characterized by aggressive metastatic behavior and resistance to chemotherapy, affecting approximately 40% of cases worldwide [1]. Despite advances in immunotherapy, LUAD presents considerable clinical challenges due to its metastatic potential and frequent chemotherapy resistance [2,3].

Epithelial-mesenchymal transition (EMT) is a critical driver of LUAD progression and therapeutic resistance [4]. The pleckstrin-homology-like domain family-A member 2 (PHLDA2), located within the imprinted 11p15.5 region, has been increasingly implicated in several cancer types, including breast, pancreatic, and osteosarcoma. However, its role and transcriptional regulation in LUAD remain unclear [5]. Bioinformatic analysis of the PHLDA2 promoter using the JASPAR-2022 database revealed a high-affinity binding motif for ETS-like-1 protein (ELK1), a member of the E26 transformation-specific (ETS) transcription factor family that is frequently activated in cancer and regulates genes governing proliferation, differentiation, apoptosis, and EMT [6,7]. Given this evidence, we therefore hypothesized that ELK1 directly upregulates PHLDA2 expression, thereby promoting LUAD progression. Furthermore, PHLDA2 has been associated with activation of the phosphoinositide 3-kinase/protein kinase B/mechanistic target of rapamycin (PI3K/AKT/mTOR) pathway and chemoresistance in other tumor types [8]. Although this link remains uninvestigated in LUAD, it provides a mechanistic context that warrants further investigation.

In this study, we investigated PHLDA2 expression and its prognostic significance in LUAD, the impact of PHLDA2 knockdown on malignant phenotypes and cisplatin sensitivity, and the regulatory link between ELK1 and PHLDA2. Our findings identify the PHLDA2/ELK1 axis as a potential driver of LUAD progression.

Materials and Methods

Cell Lines and Culture

A549 (ATCC CCL-185, KRASG12S, EGFR/ALK WT, ATCC, Manassas, VA, USA) and PC9 (RIKEN RCB4455, EGFR exon-19 deletion, RIKEN Cell Bank, Tsukuba, Japan) LUAD cell lines, along with HEK293T cells (ATCC CRL-11268, ATCC), were cultured in Dulbecco's Modified Eagle Medium (DMEM) (Gibco, Cat. No.11965092, Waltham, MA, USA) supplemented with 10 % fetal bovine serum (FBS; Gibco, Cat. No.10270, Waltham, MA, USA) at 37 °C in a humidified environment containing 5% CO_2. All cell lines were authenticated using short tandem repeat (STR) (December 2024) to confirm their identity and were found to be free of mycoplasma contamination using the Universal Mycoplasma Detection Kit (ATCC, Cat. No.30-1012K). The growth medium was refreshed every 48 hours, and cells were regularly passaged to maintain exponential growth.

In Silico PHLDA2 Expression Analysis

PHLDA2 transcriptional expression data were extracted from the gene expression profiling interactive analysis (GEPIA; http://gepia.cancer-pku.cn/) database, which combines RNA-seq datasets from The Cancer Genome Atlas-Lung Adenocarcinoma (TCGA-LUAD, n = 483) cohort and normal lung tissues from the genotype tissue expression (GTEx, n = 347). Gene-level expression was assessed as transcripts per million (TPM), followed by $\log_2$ transformation [$\log_2$(TPM+1)] to stabilize variance and estimate a normal distribution. Differential expression analysis between tumor and normal tissues was conducted using the non-parametric Mann–Whitney U test. Findings were presented as box plots generated through the GEPIA interface, and significance was achieved at a *p*-value of less than 0.05.

In Silico Promoter Analysis (JASPAR-2022)

Putative ELK1-binding motifs within the *PHLDA2* promoter region were identified using the JASPAR-2022 database (http://jaspar.genereg.net). Motif scanning was conducted with the ELK1 transcription factor profile (MA0028.2) from the vertebrates' collection, employing a relative profile score threshold of ≥85% to ensure high-confidence binding site identification. The identified candidate sites were then used to design primers for chromatin immunoprecipitation, followed by quantitative polymerase chain reaction (chromatin immunoprecipitation-quantitative polymerase chain reaction, ChIP-qPCR) to validate ELK1 and to generate promoter fragments for cloning into luciferase constructs. The sequence of promoter could be found in the **Supplementary Materials**.

Survival Analysis

Overall survival (OS) data for LUAD patients (n = 478, 239 for each group) were retrieved from the TCGA-LUAD dataset. Patients were stratified into low-expression and high-expression groups based on the median levels of PHLDA2 expression. Kaplan–Meier (KM) survival curves were plotted, and statistical significance between groups was determined using the log-rank test. Furthermore, hazard ratios (HRs) with 95% confidence intervals (CIs) were measured using univariate Cox proportional hazards regression. Multivariate adjustment for clinical covariates was not applied, and the findings therefore indicate unadjusted associations between PHLDA2 expression and OS.

PHLDA2 Knockdown by siRNA

A549 and PC9 cells were seeded in 6-well plates at a density of 1×10^5 cells per well and then transfected with 50 nM siPHLDA2 (GenePharma, 5′-GGU CAA GAA UGG CAA CAA UTT-3′) or a non-targeting negative control small interfering RNA (siRNA) (siNC; GenePharma, 5′-UUC UCC GAA CGU GUC ACG UTT-3′) using Lipofectamine 3000 (Thermo Fisher Scientific, Cat. No. L3000-015, Waltham, MA, USA), following the manufacturer's instructions. BLAST analysis was conducted to confirm that siRNA had no significant off-target homology. Forty-eight hours post-transfection, knockdown efficiency was assessed at both mRNA and protein levels using quantitative reverse transcription polymerase chain reaction (qRT-PCR) and Western blot analyses, respectively.

Cell Viability Assay

Cellular viability was determined using the cell counting kit-8 (CCK-8) assay (Dojindo Laboratories, Cat. No. CK04, Kumamoto, Japan). After siRNA transfection, A549 and PC9 cells were plated into 96-well plates at a density of 5×10^3 cells per well in 100 µL of DMEM. CCK-8 reagent (10 µL) was added to each well at 24-, 48-, and 72-hour post-transfection, followed by a 2-hour incubation at 37 °C. Absorbance was measured at 450 nm using a microplate reader. Finally, cell viability was determined using the following formula: Cell Viability (%) = $[(OD_{treat} - OD_{blank}) / (OD_{ctrl} - OD_{blank})] \times 100\%$. OD, optical density.

Colony Formation Assay

To assess long-term proliferative capacity, colony formation assays were performed. After siRNA transfection, A549 and PC9 cells were seeded into 6-well plates at a density of 500 cells per well and cultured for 14 days, with the media refreshed every 3 days. Following incubation, colonies were fixed with paraformaldehyde, stained, and those containing over 50 cells were counted as positive colonies. Colony counts were performed independently by blinded observers, and findings were presented as the average number of colonies per well from triplicate experiments.

Apoptosis Assay

Apoptosis was assessed with flow cytometry using the Annexin V-fluorescein isothiocyanate (FITC)/propidium iodide (PI) Apoptosis Detection Kit (BD Biosciences, Cat. No. 556547, Franklin Lakes, NJ, USA). Forty-eight hours following transfection with either siNC or siPHLDA2, A549 and PC9 cells were harvested, washed twice with cold phosphate-buffered saline (PBS), and resuspended in 100 µL of binding buffer. After that, 5 µL of Annexin V-FITC and 5 µL of PI were added to each sample and then incubated for 15 minutes at room temperature in the dark. Samples were analyzed using a BD FACSCanto™ II Clinical Flow Cytometry System (BD Biosciences, Franklin Lakes, NJ, USA).

Transwell Migration and Invasion Assays

Cell migration and invasion assays were conducted using 24-well Transwell inserts (Corning, Cat. No. 3422, New York, NY, USA) with an 8-µm pore membrane. For migration assays, 1×10^4 cells suspended in serum-free medium were seeded into the upper chamber, while the lower chamber was filled with DMEM containing 10% FBS to serve as a chemoattractant. After 24 hours of incubation, non-migrated cells were removed with a sterile cotton swab. Cells that had migrated to the underside of the membrane were fixed with 4% paraformaldehyde, stained with 0.1% crystal violet, and quantified by counting in five randomly selected fields at 100× magnification. For invasion assays, the upper chamber of the inserts was pre-coated with Matrigel (Corning, Cat. No. 356234; diluted 1:5 in serum-free DMEM). Cells were seeded and allowed to invade for 48 hours, followed by fixation, staining, and quantification using the same protocol as applied to migration assays.

Western Blot Analysis of EMT Markers

Cells were lysed using RIPA buffer (Beyotime, Cat. No. P0013C, Shanghai, China) containing protease and phosphatase inhibitors to maintain protein integrity. Equal amounts of total protein (30 µg per sample) were separated via sodium dodecyl sulfate–polyacrylamide gel electrophoresis (SDS-PAGE) and then transferred onto polyvinylidene difluoride (PVDF) membranes. All antibodies used in this experiment were obtained from Proteintech (Rosemont, IL, USA). Primary antibodies applied in WB analysis were as follows: matrix metalloproteinase-2 (MMP-2) (Cat. No. 10373-2-AP, 1:1000), MMP-9 (Cat. No. 10375-2-AP, 1:1000), E-cadherin (Cat. No. 20874-1-AP, 1:1000), N-cadherin (Cat. No. 22018-1-AP, 1:1000), alpha-smooth muscle actin (α-SMA) (Cat. No. CL594-14395, 1:1000), and glyceraldehyde-3-phosphate dehydrogenase (GAPDH) (Proteintech, 60004-1-Ig, 1:5000), which served as a loading control. Membranes were blocked with 5% non-fat dry milk for one hour at room temperature, followed by incubation with primary antibodies overnight at 4 °C. The next day, membranes were washed and incubated with horseradish peroxidase (HRP)-conjugated goat anti-rabbit (Proteintech, Cat. No. SA00001-2, 1:5000) or anti-mouse (Cat. No. SA00001-1, 1:5000) secondary antibodies for 1 hour at room temperature. Protein bands were observed using the SuperSignal West Femto (Thermo Fisher Scientific), and immunoblot images were captured with a Bio-Rad ChemiDoc MP system. Protein band intensities were quantified using ImageJ (National Institutes of Health, Version 1.54p, Bethesda, MD, USA) software and normalized first to GAPDH and then to the control group (set to 1.0) for relative quantification.

Cisplatin Sensitivity Assay

A549 and PC9 cells transfected with either siNC or siPHLDA2 were exposed to varying concentrations (0, 0.5, 1, 1.5, 2, 2.5 µM) of cisplatin (Sigma-Aldrich, Cat. No. P4394) for 48 hours. This selected sub-lethal dose range was applied to avoid acute cytotoxic saturation while enabling reliable estimation of the half-maximal inhibitory concentration (IC_{50}). After treatment, cell viability was determined using the CCK-8 assay, as described above.

Chromatin Immunoprecipitation (ChIP) Assay

Chip assays were conducted using the EZ-Magna ChIP assays kit (Millipore, Cat. No. 17-408, Burlington, MA, USA), following the manufacturer's instructions. Briefly, A549 cells (1×10^7) were fixed with 1% formaldehyde for 10 minutes at room temperature. Cells were lysed, and chromatin was fragmented by sonication to yield DNA fragments ranging from 200–500 bp. Immunoprecipitation was performed with an anti-ELK1 antibody (Cell Signaling Technology, Cat. No. CST 9192, Danvers, MA, USA; 1:100) or control immunoglobulin G (IgG). The precipitated DNA was quantified by qPCR using primers specific to the PHLDA2 promoter (F 5′-AGCCACAGAGGTGGGACTTT-3′, R 5′-CAGGAGGACTCAGGGTGACA-3′). ELK1 binding was normalized to the input DNA and expressed as a percentage using the following formula: $\%\text{Input} = 2^{\text{Ct (Adjusted Input)} - \text{Ct (ChIP)}} \times 100$. Enrichment was assessed as fold change relative to IgG controls (ELK1/IgG).

Dual-Luciferase Reporter Assay

The human PHLDA2 promoter (–896/+104) was amplified and cloned into the pGL3-basic vector using XhoI and HindIII restriction sites. The full-length ELK1 coding sequence (NM_005229) was inserted into the pcDNA3.1(+) expression vector. For luciferase reporter assays, A549 cells were seeded into 24-well plates and co-transfected with 0.5 µg of PHLDA2-Luc, 0.05 µg of pRL-TK (internal control), and 0.5 µg of either ELK1-pcDNA3.1(+) or empty vector using Lipofectamine 3000 (Thermo Fisher Scientific, Cat. No. L3000-015, Waltham, MA, USA). After 48 hours of transfection, luciferase activity was measured using the Dual-Luciferase Reporter As-

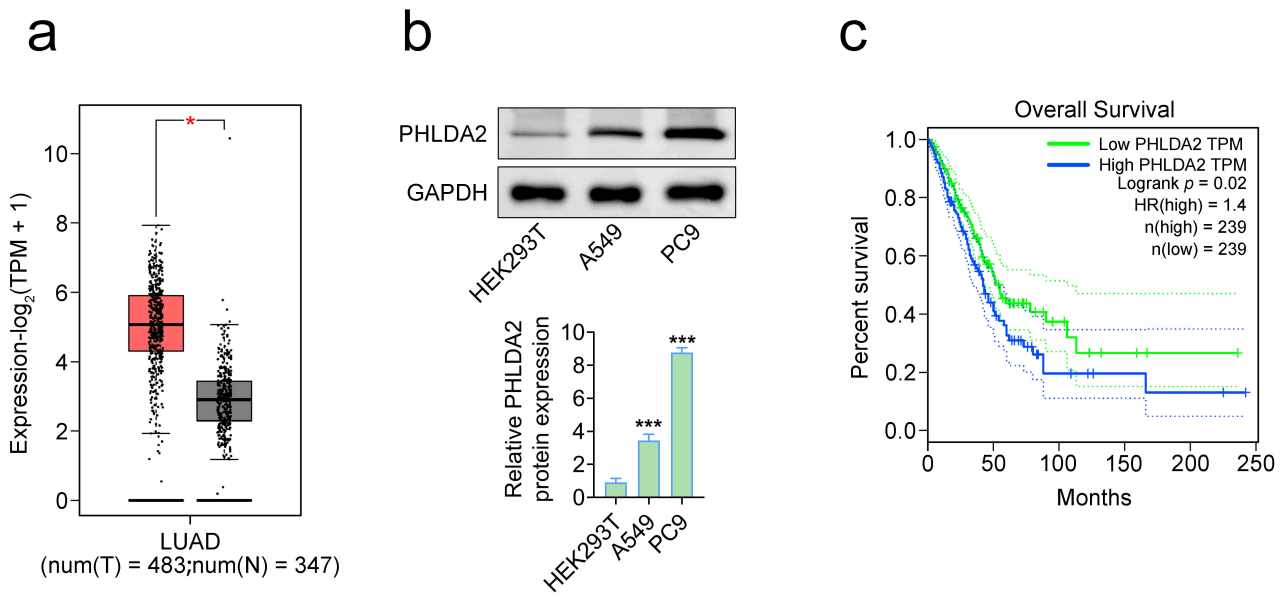

Fig. 1. PHLDA2 expression and prognosis in LUAD. (a) GEPIA comparison of TCGA-LUAD tumor samples (red, n = 483) compared to GTEx normal lung (grey, n = 347). (b) Western blot analysis of PHLDA2 in HEK293T, A549, PC9 (n = 3). (c) Kaplan–Meier OS analysis in TCGA-LUAD (n = 478, 239 for each group). *$p < 0.05$, ***$p < 0.001$ compared to the HEK293T group. PHLDA2, pleckstrin-homology-like domain family-A member 2; LUAD, lung adenocarcinoma; GEPIA, gene expression profiling interactive analysis; TCGA-LUAD, The Cancer Genome Atlas–Lung Adenocarcinoma; OS, overall survival; GAPDH, glyceraldehyde-3-phosphate dehydrogenase; TPM, transcripts per million.

say System (Promega, Cat. No. E1910, Madison, WI, USA) and normalized to Renilla luciferase levels. Relative promoter activity was determined as $(\text{Firefly/Renilla})_{\text{sample}} / (\text{Firefly/Renilla})_{\text{control}}$.

Statistical Analysis

Statistical analysis was performed using Statistical Package for the Social Sciences (IBM, SPSS version 22.0, New York, NY, USA) software, and data were expressed as mean ± standard deviation (SD) from at least three independent experiments. Normality in data distribution was evaluated using the Shapiro–Wilk test. For comparisons between two groups, either the unpaired *t*-test (for normally distributed data) or the Mann–Whitney U test (for non-parametric data) was used. For multiple groups, one-way analysis of variance (ANOVA) followed by Tukey's post-hoc or Kruskal–Wallis test with Dunn's correction was applied, as appropriate. Dose–response relationship was modeled using a four-parameter logistic regression. The IC_{50} and its 95% confidence interval (CI) were obtained from the model fit, and group differences in IC_{50} were evaluated using an extra-sum-of-squares F-test on globally fitted curves. For apoptosis assays and other multi-group comparisons, one-way ANOVA with Tukey's post-hoc test was used. Statistical significance was determined at a *p*-value of <0.05.

Results

PHLDA2 Is Overexpressed in LUAD

PHLDA2 was significantly upregulated in LUAD tumor samples (red, n = 483) than in normal lung tissues (grey, n = 347) ($p < 0.05$; Fig. 1a). Similarly, Western blot analysis confirmed higher PHLDA2 protein levels in A549 and PC9 cells compared to the HEK293T control (normalized to 1; Fig. 1b). Kaplan-Meier survival analysis revealed that patients with high PHLDA2 expression showed substantially poorer overall survival compared to those with low expression (log-rank $p = 0.02$; Fig. 1c).

PHLDA2 Knockdown Inhibits LUAD Cell Growth

Manipulation of PHLDA2 expression altered the growth and apoptosis of LUAD cells. Western blotting confirmed successful PHLDA2 overexpression and knockdown (siPHLDA2) in A549 and PC9 cells, with control and siNC groups demonstrating comparable basal levels (Fig. 2a). Cell Counting Kit-8 (CCK-8) assays revealed that PHLDA2 knockdown substantially reduced cell viability relative to both control groups ($p < 0.05$), whereas PHLDA2 overexpression increased viability ($p < 0.05$, Fig. 2b). Consistently, colony formation assays demonstrated a significant decrease in the number of colonies (≥50 cells) after siPHLDA2 transfection ($p < 0.05$), whereas overexpression of PHLDA2 substantially increased the number of colonies compared to control/siNC

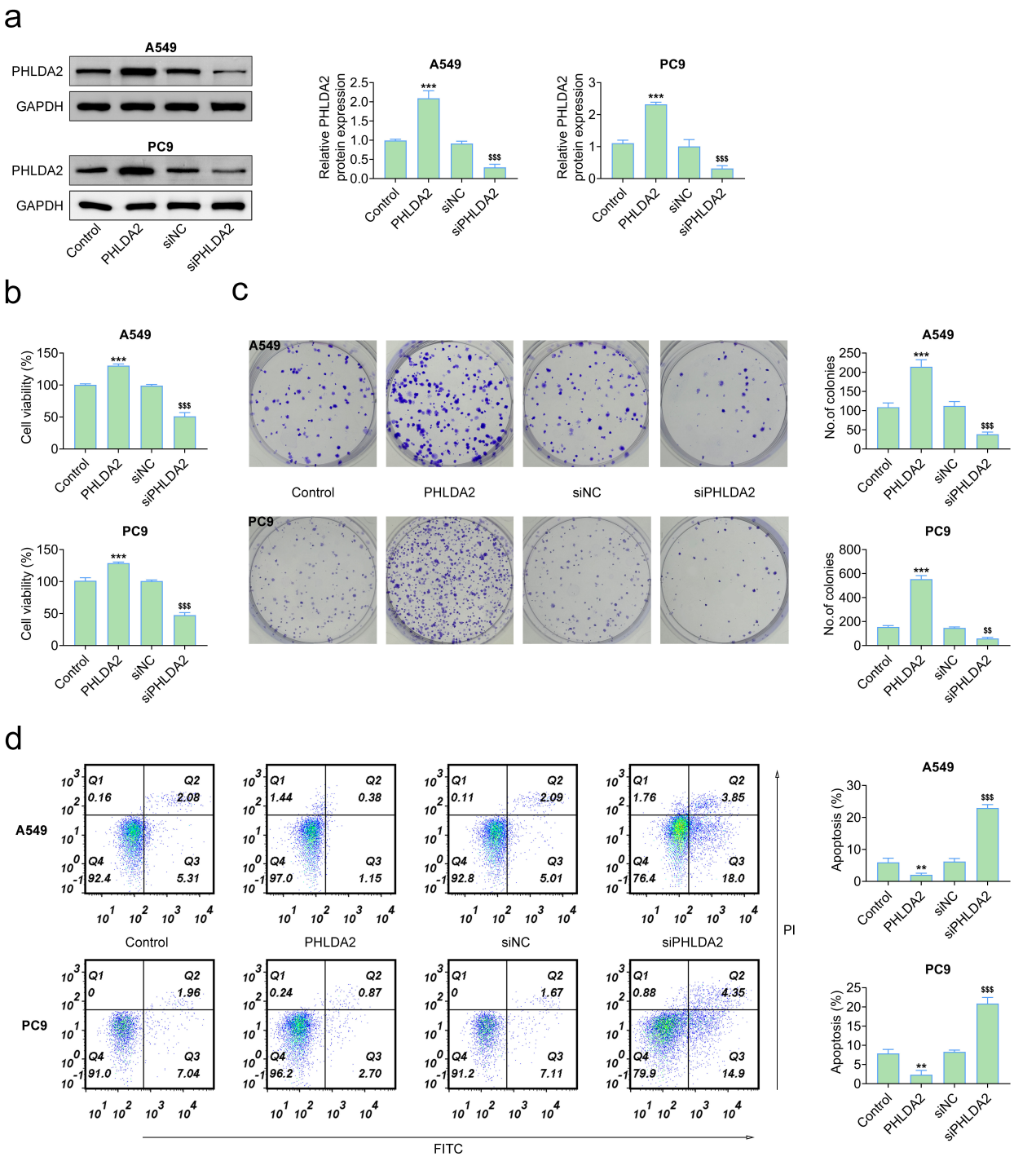

Fig. 2. Impact of PHLDA2 overexpression and knockdown on LUAD cell growth and apoptosis. (a) WB validation of siPHLDA2. (b) CCK-8 cell viability (%) over 72 hours (n = 3). (c) Colony formation (≥50 cells) per well after 14 days (n = 3). (d) Annexin V/PI apoptosis (n = 3). $^{**}p < 0.01$, $^{***}p < 0.001$ compared to the control group; $^{\$\$}p < 0.01$, $^{\$\$\$}p < 0.001$ compared to the siNC group. WB, Western blot; siPHLDA2, silencing PHLDA2; CCK-8, cell counting kit-8.

($p < 0.05$, Fig. 2c). Moreover, flow cytometry showed a higher proportion of apoptotic cells in the siPHLDA2 group ($p < 0.05$) and reduced apoptosis in PHLDA2-overexpression cells relative to the control/siNC group ($p < 0.05$, Fig. 2d).

PHLDA2 Knockdown Suppresses EMT and Invasion in LUAD Cells

The effect of PHLDA2 silencing on the migratory and invasive capability of LUAD cells was assessed using Transwell assays. In three independent experiments (scale bar

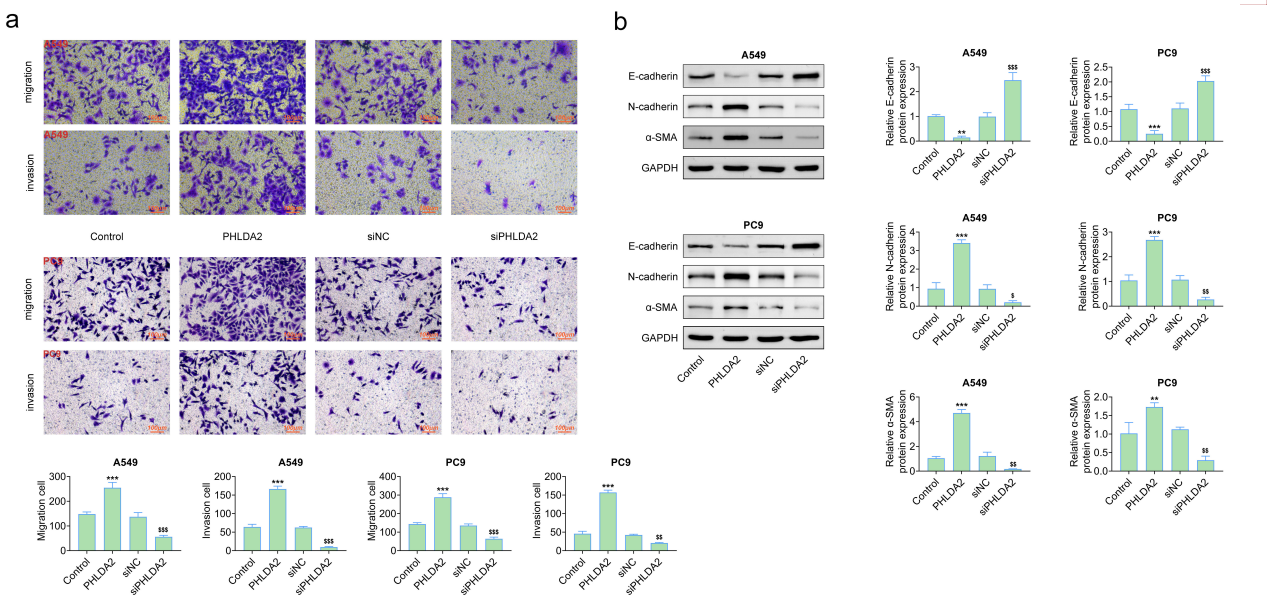

Fig. 3. Effect of PHLDA2 knockdown on Migration, invasion, and EMT. (a) Transwell migration (24 hours) and Matrigel invasion (48 hours); scale bar = 100 μm; n = 3. (b) WB analysis of E-cadherin, N-cadherin, and α-SMA with densitometry (n = 3). $^{**}p < 0.01$, $^{***}p < 0.001$ compared to the control group; $^{\$}p < 0.05$, $^{\$\$}p < 0.01$, $^{\$\$\$}p < 0.001$ compared to the siNC group. EMT, epithelial-mesenchymal transition; α-SMA, alpha-smooth muscle actin.

= 100 μm), siPHLDA2-treated A549 and PC9 cells exhibited approximately 50 % fewer migrated cells than either untreated or siNC controls ($p < 0.05$). However, a more pronounced reduction was observed in Matrigel-coated inserts, where invasion dropped by >60 % ($p < 0.001$ and $p < 0.05$, Fig. 3a). Consistent with these functional effects, WB densitometry (n = 3) revealed a 2- to 3-fold increase in the epithelial marker E-cadherin ($p < 0.05$), accompanied by substantial downregulation of the mesenchymal proteins N-cadherin and α-SMA ($p < 0.05$) in siPHLDA2 cells (Fig. 3b). Collectively, these results indicate that PHLDA2 knockdown inhibits EMT, thereby shifting LUAD cells toward a more epithelial and less invasive phenotype.

PHLDA2 Knockdown Enhances Sensitivity to Cisplatin

PHLDA2 modulates the sensitivity of LUAD cells to cisplatin treatment. Dose-response modelling (0–2.5 μM, 48 hours) showed that PHLDA2 overexpression shifted the curve to the right, indicating an elevated IC_{50} relative to cisplatin alone, whereas PHLDA2 silencing (siPHLDA2) shifted the curve to the left, indicating enhanced sensitivity and a lower IC_{50} relative to cisplatin + siNC ($p < 0.05$; Fig. 4a). The corresponding bar charts summarize the IC_{50} values (±95% CI) for each group. Consistently, treatment with a single 10 μM cisplatin dose induced considerably greater apoptosis in siPHLDA2-transfected cells and reduced apoptosis in PHLDA2-overexpressing cells compared with their respective controls ($p < 0.05$; Fig. 4b).

ELK1 Activates PHLDA2 Transcription in LUAD Cells

To explore the transcriptional regulation of PHLDA2 in LUAD cells, we examined the role of ELK1, a transcription factor involved in tumor progression. Western blot analysis was performed to assess ELK1 and PHLDA2 protein levels in A549 and PC9 cells under different experimental conditions, including control, ELK1 overexpression, and knockdown via siRNA. ELK1 overexpression (ELK1 OE) significantly increased PHLDA2 protein levels, whereas ELK1 knockdown (siELK1) reduced its expression levels ($p < 0.05$; Fig. 5a).

Correlation analysis using the GEPIA database showed a substantial positive association between PHLDA2 and ELK1 expression levels in LUAD tissues, indicating a functional relationship (Fig. 5b). Additionally, in silico analysis with the JASPAR database identified a potential ELK1 binding site within the PHLDA2 promoter region (Fig. 5c).

ChIP-qPCR revealed significant enrichment of ELK1 at the PHLDA2 promoter compared with IgG control ($p < 0.05$; Fig. 5d). Similarly, dual-luciferase assays demonstrated that ELK1 overexpression increased PHLDA2 promoter activity ($p < 0.05$), whereas silencing ELK1 (siELK1) inhibited this activity ($p < 0.05$) compared to vector or siNC controls (Fig. 5e). Functionally, siELK1 reduced both cell viability ($p < 0.05$) and colony formation ($p < 0.05$), while ELK1 overexpression produced the opposite effects (Fig. 5f,g). These observations support a model in which ELK1 activates PHLDA2 transcription, thereby promoting the growth and survival of LUAD cells.

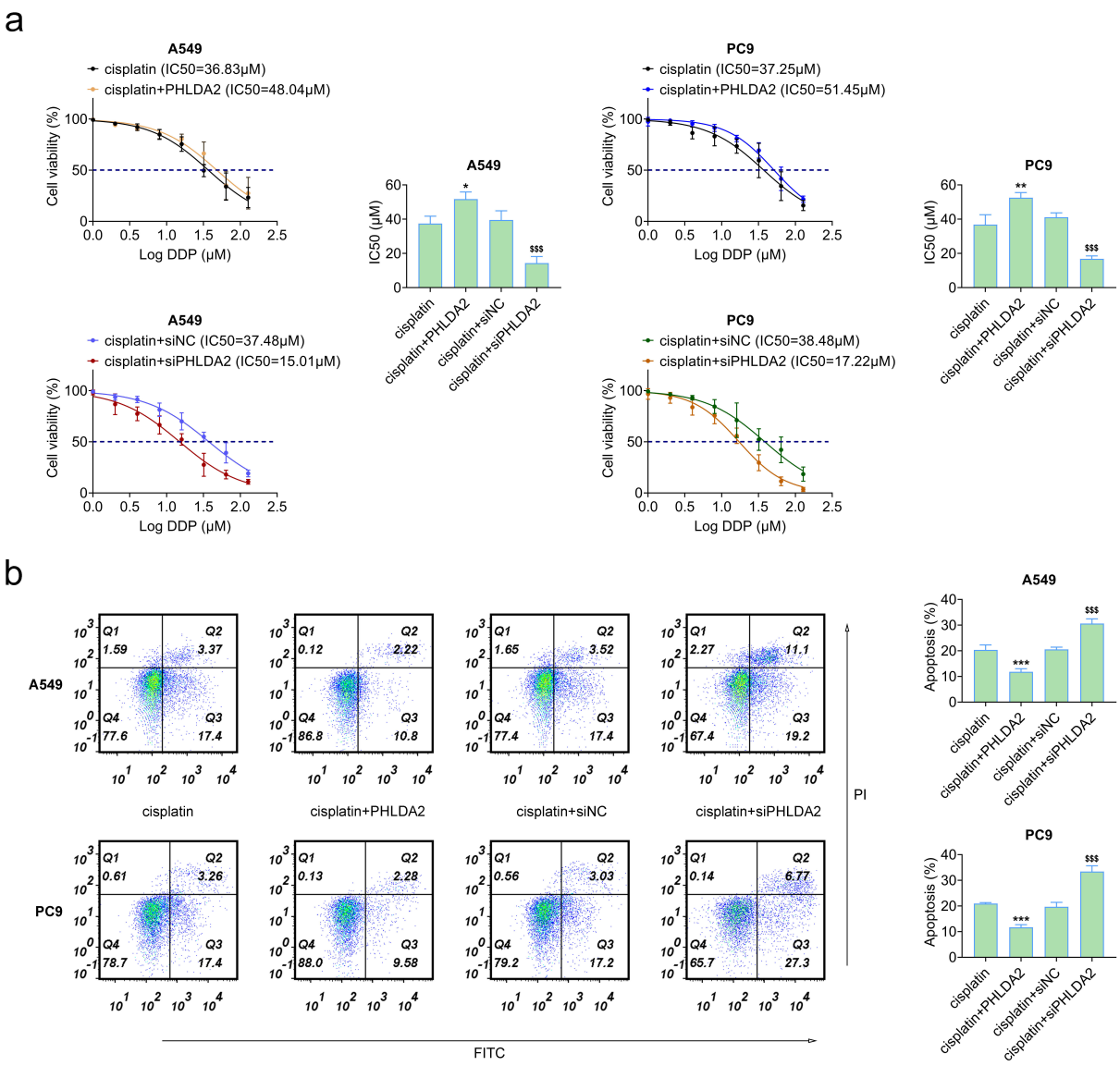

Fig. 4. PHLDA2 regulates the sensitivity and apoptosis of LUAD cells to cisplatin exposure. (a) Cisplatin dose–response curves (0–2.5 μM, 48 hours) in A549 and PC9 under cisplatin only, cisplatin + PHLDA2 overexpression (PHLDA2), cisplatin + siNC, and cisplatin + siPHLDA2. Right panels: IC_{50} (±95% CI) from four-parameter logistic fits; between-group differences by extra-sum-of-squares F-test. Y-axis: Cell viability (%). (b) Annexin V/PI flow cytometry following 10 μM cisplatin treatment. Bars show mean ± SD; one-way ANOVA followed by Tukey post-hoc (n = 3). *$p < 0.05$, **$p < 0.01$, ***$p < 0.001$ compared to the control group; $^{\$\$\$}p < 0.001$ compared to the cisplatin + siNC group.

Discussion

This study identifies PHLDA2 as a putative oncogenic driver in LUAD. Both bioinformatic analysis and experimental validation demonstrated that PHLDA2 is upregulated in tumor tissues, correlates with poor prognosis, and enhances malignant phenotypes *in vitro*. Silencing PHLDA2 reversed EMT, suppressed invasion, and increased cisplatin sensitivity, which is consistent with previous findings that EMT confers chemoresistance [9]. Furthermore, we report that ELK1 directly binds to the PHLDA2 promoter and activates its transcription, thereby expanding the spectrum of ELK1-regulated genes linked to LUAD progression [8].

PHLDA2 has been reported as an oncogenic driver in several cancer types, including breast [10], pancreatic [11], and osteosarcoma [12]. In LUAD, PHLDA2 levels were found to be significantly upregulated compared to normal lung tissues. Survival analyses further confirmed that this overexpression is associated with poor prognosis, with elevated PHLDA2 levels correlating with reduced overall survival, indicating its crucial role in LUAD progression and metastasis [5].

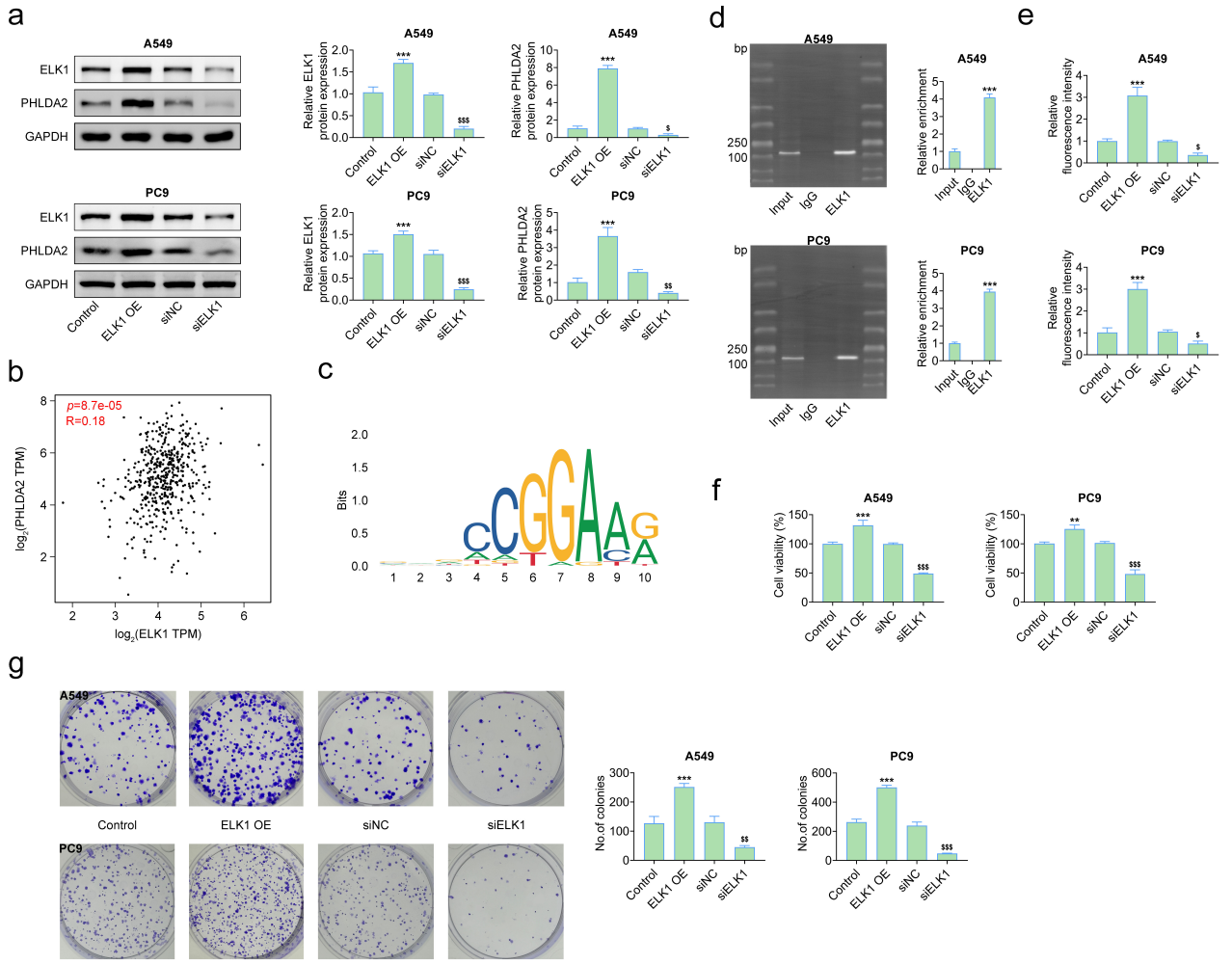

Fig. 5. Impact of ELK1 on PHLDA2 transcription. (a) WB analysis of ELK1 OE/siELK1 and PHLDA2 (n = 3). (b) GEPIA correlation in LUAD tumors. (c) Predicted ELK1 motif (JASPAR-2022). (d) ChIP-qPCR enrichment at the PHLDA2 promoter (n = 3). (e) Luciferase activity from PHLDA2-Luc under ELK1 OE/knockdown (n = 3). (f) Cell viability (%) after ELK1 modulation (n = 3). (g) Colony formation with ELK1 OE/knockdown (n = 3). $^{**}p < 0.01$, $^{***}p < 0.001$ compared to the control group, $^{\$}p < 0.05$, $^{\$\$}p < 0.01$, $^{\$\$\$}p < 0.001$ compared to the siNC group. ELK1, ETS-like-1 protein, a transcription factor of the ETS family.

The oncogenic potential of PHLDA2 is attributed to its role in driving EMT, a crucial process in cancer metastasis. EMT enables epithelial cells to acquire mesenchymal traits, thereby increasing their migratory and invasive capabilities. In our study, PHLDA2 knockdown reversed EMT in LUAD cells, as evidenced by increased E-cadherin expression and decreased levels of mesenchymal markers, including N-cadherin and α-SMA. This molecular shift was accompanied by reduced migration and invasion, further supporting the role of PHLDA2 in promoting metastasis [13,14]. Notably, the involvement of PHLDA2 in EMT is consistent with findings in other cancers, where it has been found to facilitate metastatic dissemination through interaction with key EMT regulators. For example, PHLDA2 has been shown to activate the PI3K/Akt and mTOR pathways, which are critical for cell growth, survival in cancer [13,15]. These signaling pathways are known to enhance the EMT process, suggesting that PHLDA2 may act upstream of these signaling pathways to drive EMT and thereby promote LUAD progression and malignancy.

One of the most clinically significant findings of this study is the role of PHLDA2 in mediating resistance to cisplatin, a commonly used chemotherapy agent for LUAD [16]. Chemoresistance remains a major challenge in LUAD treatment, often leading to poor therapeutic outcomes and disease relapse. Our results demonstrated that PHLDA2 knockdown significantly increased the sensitivity of LUAD cells to cisplatin, as evidenced by reduced IC_{50} values and increased apoptosis following cisplatin treatment. The well-established association between EMT and chemoresistance provides a mechanistic explanation for this effect. As EMT not only promotes metastasis but also confers resistance to apoptosis, thereby alleviating cancer cell responsiveness to chemotherapy. By promoting EMT, PHLDA2

likely contributes to cisplatin resistance in LUAD. This is consistent with observations from other cancers, including breast and pancreatic cancers, where EMT has been linked to resistance to various chemotherapeutic agents [17,18].

Notably, the role of PHLDA2 in chemoresistance may extend beyond EMT, involving modulation of apoptotic pathways. In our study, PHLDA2 silencing substantially elevated apoptosis in LUAD cells, indicating that PHLDA2 protects tumor cells from cisplatin-induced cell death by suppressing pro-apoptotic signaling. Supporting this, previous studies have reported that PHLDA2 modulates the expression of key apoptotic regulators, including Bcl-2 and Bax, in other cancers [19,20].

The transcription factor ELK1 plays a crucial role in regulating the expression of genes involved in cell proliferation, differentiation, and survival. In this study, we identified ELK1 as a direct regulator of PHLDA2 transcription in LUAD cells [21]. Both ChIP and dual-luciferase reporter assays confirmed that ELK1 binds to the PHLDA2 promoter and activates its transcription. These results emphasize the ELK1/PHLDA2 axis as a critical regulatory node that promotes LUAD progression. Pharmacologically disrupting this axis may therefore curb tumor growth and metastasis.

Mechanistically, sustained PHLDA2 expression may promote cisplatin resistance by upregulating drug-efflux pumps such as MDR1/ABCB1 [22] and by maintaining high levels of anti-apoptotic proteins like Bcl-2, which inhibits mitochondrial apoptosis and supports platinum tolerance [23]. These hypotheses are consistent with our findings, where PHLDA2 knockdown reverses EMT and significantly alleviates the cisplatin IC_{50} *in vitro*.

ELK1 is frequently activated in cancers and has been shown to promote tumorigenesis by regulating genes involved in EMT, migration, and invasion. Our findings suggest that ELK1 may drive LUAD malignancy, at least in part, by upregulating PHLDA2 expression, which has implicated ELK1 in the progression of lung cancer and other malignancies [24]. Targeting the ELK1/PHLDA2 axis may therefore provide a new treatment approach for inhibiting LUAD progression and overcoming metastasis and drug resistance.

Despite these promising outcomes, we acknowledge several limitations in our study, which also underscore avenues for future research. (i) All functional assays were performed *in vitro* using only two LUAD cell lines; validation in xenograft or patient-derived models will be required to confirm the activity of the ELK1/PHLDA2 pathways *in vivo*. (ii) Survival analyses were limited to univariate, median-based comparisons; more robust multivariable Cox modeling with alternative cut-points will be needed to establish PHLDA2 as an independent prognostic marker. (iii) Although the ELK1–PHLDA2 correlation in TCGA LAUD samples was statistically significant, it was weak ($r = 0.18$) and derived from a single dataset; independent validation in additional LUAD cohorts, particularly stratified by EGFR/KRAS driver status, is warranted. (iv) ChIP-qPCR was performed only in A549 cells without a non-target promoter control; extending these assays to PC9 cells and including an unrelated promoter primer would confirm binding specificity across genetic backgrounds. (v) Functional knockdown experiments relied on a single siRNA sequence; rescue experiments and the use of additional siPHLDA2 sequences will help exclude off-target effects. (vi) The cisplatin dose range applied (0–2.5 µM) captured sub-lethal effects but does not fully replicate clinical exposures; extending dose-response curves up to 10 µM is ongoing. Finally, testing PI3K/AKT/mTOR inhibitors in the context of PHLDA2 modulation will clarify whether this pathway mediates its oncogenic effects. Addressing these limitations will refine and enhance the therapeutic potential of targeting the ELK1/PHLDA2 axis in LUAD.

Conclusion

PHLDA2 knockdown suppresses malignant phenotypes and increases cisplatin sensitivity in LUAD cells, whereas ELK1 activates PHLDA2 transcription. These findings reveal the ELK1/PHLDA2 axis as a promising therapeutic target, warranting further validation in *in vivo* models and clinical settings.

Availability of Data and Materials

All data generated or analyzed during this study are included in this published article. The datasets used and/or analyzed during the present study are available from the corresponding author on reasonable request.

Author Contributions

Both authors contributed to the study conception and design. Material preparation and the experiments were performed by FM. Data collection and analysis were performed by DZ. The first draft of the manuscript was written by FM and both authors critically revised previous versions of the manuscript. Both authors read and approved the final manuscript. Both authors have participated sufficiently in the work and agreed to be accountable for all aspects of the work.

Ethics Approval and Consent to Participate

Not applicable.

Acknowledgment

Not applicable.

Funding

This research received no external funding.

Conflict of Interest

The authors declare no conflict of interest.

Supplementary Material

Supplementary material associated with this article can be found, in the online version, at https://doi.org/10.24976/Discov.Med.202537202.216.

References

[1] Duma N, Santana-Davila R, Molina JR. Non-Small Cell Lung Cancer: Epidemiology, Screening, Diagnosis, and Treatment. Mayo Clinic Proceedings. 2019; 94: 1623–1640. https://doi.org/10.1016/j.mayocp.2019.01.013.

[2] Pan Z, Wang K, Wang X, Jia Z, Yang Y, Duan Y, *et al*. Cholesterol promotes EGFR-TKIs resistance in NSCLC by inducing EGFR/Src/Erk/SP1 signaling-mediated ERRα re-expression. Molecular Cancer. 2022; 21: 77. https://doi.org/10.1186/s12943-022-01547-3.

[3] Moldvay J, Tímár J. KRASG12C mutant lung adenocarcinoma: unique biology, novel therapies and new challenges. Pathology and Oncology Research. 2024; 29: 1611580. https://doi.org/10.3389/pore.2023.1611580.

[4] Cui Y, Wang X, Zhang L, Liu W, Ning J, Gu R, *et al*. A novel epithelial-mesenchymal transition (EMT)-related gene signature of predictive value for the survival outcomes in lung adenocarcinoma. Frontiers in Oncology. 2022; 12: 974614. https://doi.org/10.3389/fonc.2022.974614.

[5] Baldavira CM, Machado-Rugolo J, Prieto TG, Bastos DR, Balancin M, Ab'Saber AM, *et al*. The expression patterns and prognostic significance of pleckstrin homology-like domain family A (PHLDA) in lung cancer and malignant mesothelioma. Journal of Thoracic Disease. 2021; 13: 689–707. https://doi.org/10.21037/jtd-20-2909.

[6] Hou CH, Lin FL, Hou SM, Liu JF. Cyr61 promotes epithelial-mesenchymal transition and tumor metastasis of osteosarcoma by Raf-1/MEK/ERK/Elk-1/TWIST-1 signaling pathway. Molecular Cancer. 2014; 13: 236. https://doi.org/10.1186/1476-4598-13-236.

[7] Su T, Zhang N, Wang T, Zeng J, Li W, Han L, *et al*. Super Enhancer-Regulated LncRNA LINC01089 Induces Alternative Splicing of DIAPH3 to Drive Hepatocellular Carcinoma Metastasis. Cancer Research. 2023; 83: 4080–4094. https://doi.org/10.1158/0008-5472.CAN-23-0544.

[8] Ma Z, Lou S, Jiang Z. PHLDA2 regulates EMT and autophagy in colorectal cancer via the PI3K/AKT signaling pathway. Aging. 2020; 12: 7985–8000. https://doi.org/10.18632/aging.103117.

[9] Zhou X, Han J, Zuo A, Ba Y, Liu S, Xu H, *et al*. THBS2 + cancer-associated fibroblasts promote EMT leading to oxaliplatin resistance via COL8A1-mediated PI3K/AKT activation in colorectal cancer. Molecular Cancer. 2024; 23: 282. https://doi.org/10.1186/s12943-024-02180-y.

[10] Chen Y, Takikawa M, Tsutsumi S, Yamaguchi Y, Okabe A, Shimada M, *et al*. PHLDA1, another PHLDA family protein that inhibits Akt. Cancer Science. 2018; 109: 3532–3542. https://doi.org/10.1111/cas.13796.

[11] Idichi T, Seki N, Kurahara H, Fukuhisa H, Toda H, Shimonosono M, *et al*. Molecular pathogenesis of pancreatic ductal adenocarcinoma: Impact of passenger strand of pre-miR-148a on gene regulation. Cancer Science. 2018; 109: 2013–2026. https://doi.org/10.1111/cas.13610.

[12] Li Y, Song X, Liu Z, Li Q, Huang M, Su B, *et al*. Upregulation of miR-214 Induced Radioresistance of Osteosarcoma by Targeting PHLDA2 via PI3K/Akt Signaling. Frontiers in Oncology. 2019; 9: 298. https://doi.org/10.3389/fonc.2019.00298.

[13] Liu Y, Han T, Wu J, Zhou J, Guo J, Miao R, *et al*. SPOCK1, as a potential prognostic and therapeutic biomarker for lung adenocarcinoma, is associated with epithelial-mesenchymal transition and immune evasion. Journal of Translational Medicine. 2023; 21: 909. https://doi.org/10.1186/s12967-023-04616-3.

[14] Wan Q, Zhang M, Chen W, Wang X. PHLDA2 in cancer: From molecular mechanisms to therapeutic opportunities. The Journal of Pharmacology and Experimental Therapeutics. 2025; 392: 103677. https://doi.org/10.1016/j.jpet.2025.103677.

[15] Zhang R, Sun S, Ji F, Liu C, Lin H, Xie L, *et al*. CNTN-1 Enhances Chemoresistance in Human Lung Adenocarcinoma Through Induction of Epithelial-Mesenchymal Transition by Targeting the PI3K/Akt Pathway. Cellular Physiology and Biochemistry. 2017; 43: 465–480. https://doi.org/10.1159/000480473.

[16] Feng K, Peng H, Lv Q, Zhang Y. PHLDA2 reshapes the immune microenvironment and induces drug resistance in hepatocellular carcinoma. Oncology Research. 2024; 32: 1063–1078. https://doi.org/10.32604/or.2024.047078.

[17] Hashemi M, Arani HZ, Orouei S, Fallah S, Ghorbani A, Khaledabadi M, *et al*. EMT mechanism in breast cancer metastasis and drug resistance: Revisiting molecular interactions and biological functions. Biomedicine & Pharmacotherapy. 2022; 155: 113774. https://doi.org/10.1016/j.biopha.2022.113774.

[18] Gaianigo N, Melisi D, Carbone C. EMT and Treatment Resistance in Pancreatic Cancer. Cancers. 2017; 9: 122. https://doi.org/10.3390/cancers9090122.

[19] Guo C, Liu S, Zhang T, Yang J, Liang Z, Lu S. Knockdown of PHLDA2 promotes apoptosis and autophagy of glioma cells through the AKT/mTOR pathway. Journal of Neurogenetics. 2022; 36: 74–80. https://doi.org/10.1080/01677063.2022.2096023.

[20] Jin F, Qiao C, Luan N, Li H. Lentivirus-mediated PHLDA2 overexpression inhibits trophoblast proliferation, migration and invasion, and induces apoptosis. International Journal of Molecular Medicine. 2016; 37: 949–957. https://doi.org/10.3892/ijmm.2016.2508.

[21] Li M, Lin Y, Wang J, Yang H, Ma D, Tian Y, *et al*. CREPT promotes LUAD progression by enhancing the CDK9 and RNAPII assembly to promote ERK-driven gene transcription. Theranostics. 2025; 15: 8337–8359. https://doi.org/10.7150/thno.115572.

[22] Hu Y, Cui J, Jin L, Su Y, Zhang X. LRPPRC contributes to the cisplatin resistance of lung cancer cells by regulating *MDR1* expression. Oncology Reports. 2021; 45: 4. https://doi.org/10.3892/or.2021.7955.

[23] Cho HJ, Kim JK, Kim KD, Yoon HK, Cho MY, Park YP, *et al*. Upregulation of Bcl-2 is associated with cisplatin-resistance via inhibition of Bax translocation in human bladder cancer cells. Cancer Letters. 2006; 237: 56–66. https://doi.org/10.1016/j.canlet.2005.05.039.

[24] Yang X, Zhao M, Xia M, Liu Y, Yan J, Ji H, *et al*. Selective requirement for Mediator MED23 in Ras-active lung cancer. Proceedings of the National Academy of Sciences of the United States of America. 2012; 109: E2813–E2822. https://doi.org/10.1073/pnas.1204311109.